



Missouri University of Science and Technology
Scholars' Mine

International Conferences on Recent Advances
in Geotechnical Earthquake Engineering and
Soil Dynamics

2001 - Fourth International Conference on
Recent Advances in Geotechnical Earthquake
Engineering and Soil Dynamics

30 Mar 2001, 10:30 am - 12:30 pm

Dynamic Response of Dam-Layer System to Earthquake Excitations

Sarada K. Sarma
Imperial College, London, U.K.

George Cossenas
Imperial College, London, U.K.

Follow this and additional works at: <https://scholarsmine.mst.edu/icrageesd>

 Part of the [Geotechnical Engineering Commons](#)

Recommended Citation

Sarma, Sarada K. and Cossenas, George, "Dynamic Response of Dam-Layer System to Earthquake Excitations" (2001). *International Conferences on Recent Advances in Geotechnical Earthquake Engineering and Soil Dynamics*. 13.

<https://scholarsmine.mst.edu/icrageesd/04icrageesd/session05/13>

This Article - Conference proceedings is brought to you for free and open access by Scholars' Mine. It has been accepted for inclusion in International Conferences on Recent Advances in Geotechnical Earthquake Engineering and Soil Dynamics by an authorized administrator of Scholars' Mine. This work is protected by U. S. Copyright Law. Unauthorized use including reproduction for redistribution requires the permission of the copyright holder. For more information, please contact scholarsmine@mst.edu.

DYNAMIC RESPONSE OF DAM-LAYER SYSTEM TO EARTHQUAKE EXCITATIONS

Sarada K. Sarma
Civil & Environmental Eng. Dept.
Imperial College
LONDON SW7 2BU

George Cossenas
Civil & Environmental Eng. Dept.
Imperial College
LONDON SW7 2BU

ABSTRACT

An extensive database of 'free-field' strong motion records, from rock sites all over the world, of significant strong motion (peak ground acceleration $\geq 0.1g$) has been utilised to identify the dynamic characteristics of a typical dam-layer system. Linear elastic analysis is used to calculate the response of the dam and spectra of average seismic coefficients are presented. Attenuation relationships for the response accelerations along the height of the dam are also presented and the two methods are compared. A rigid-block model is used to calculate the earthquake-induced displacements on the body of the dam, to be used as a check on safety of earth dams under seismic loading.

INTRODUCTION

The present study investigates the seismic response of a dam-soil layer system and updates the results of Ambraseys & Sarma (1967). The response of the dam is presented in terms of seismic coefficient spectra for different levels along the height of the dam. The attenuation of strong motions along the dam height is also examined and the two methods are compared. Finally the earthquake displacements on the dam are calculated and the results are compared with previous studies.

SEISMIC RESPONSE ANALYSIS

Method

The seismic response of the dam-layer system has been calculated using the method developed by Ambraseys (1960), Sarma (1979), Sarma (1981). A typical cross-section of the dam-layer system is shown in Fig. 1. Assuming that the length of the dam is great compared to its height the problem reduces to a 1-D response. The dam section is of symmetrical triangular cross-section in the transverse direction and the materials of the dam and the underlying layer are taken as homogeneous and perfectly elastic. Only distortion due to shear is considered; distortion due to bending is small for flat slopes and is consequently ignored. The dam is rigidly connected to the base and the time dependent arbitrary disturbance $\ddot{u}(t)$ acts along the base in the horizontal direction. Using the above assumptions and the initial

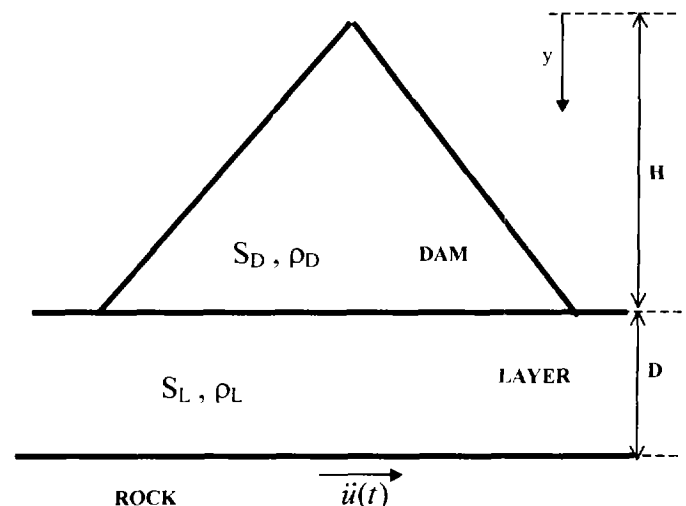


Fig. 1: Typical cross-section of the dam-layer system.

conditions of starting at rest, the absolute horizontal acceleration at a level (y) below the crest is given by :

$$a(y,t) = \sum_n \phi_n(y) S_{an} \text{ where } \phi_n(y) \text{ is a function of the}$$

geometry of the dam, S_{an} is a function of the elastic properties of the material, the amount of damping and the time history of the ground accelerations and n is the number of modes contributing to the response. The seismic coefficient, k , is defined as $k = a(y,t)/a_{max}$ where a_{max} is the maximum ground acceleration. Since for any two given levels of the dam the

accelerations obtained are neither simultaneous nor do they act in the same direction, using $a(y)_{max}$ for the calculation of the inertia forces within a sliding wedge extending along a large portion of the dam would be too conservative. An alternative way of calculating the seismic coefficient is as follows: the (predefined) sliding surface is divided into n horizontal strips, each having a mass m_i and an average seismic acceleration $k_i g$. Then, for each time instant, the total horizontal force, $F(t)$, acting on the sliding surface would be $F(t) = \sum_n m_i k_i g$ and

the average seismic coefficient given by $k(t) = F(t) / m g$, where m is the total mass of the sliding surface and g is the acceleration due to gravity. If the above process is repeated at each time step of the strong motion history, the maximum value of k can be calculated; this is the value of seismic coefficient to be used in the design. The shape of the sliding wedge is defined in a parametric form. For failure surfaces within the body of the dam, Ambraseys & Sarma (1967) have shown that sliding wedges passing through the apex of the dam and having a horizontal base are completely defined by parameter a (Fig. 2). Failure surfaces extending below the base of the dam are defined from 4 parameters, a, ψ, θ, δ . (Fig. 2). In the present study we consider the 1-parameter wedge case only.

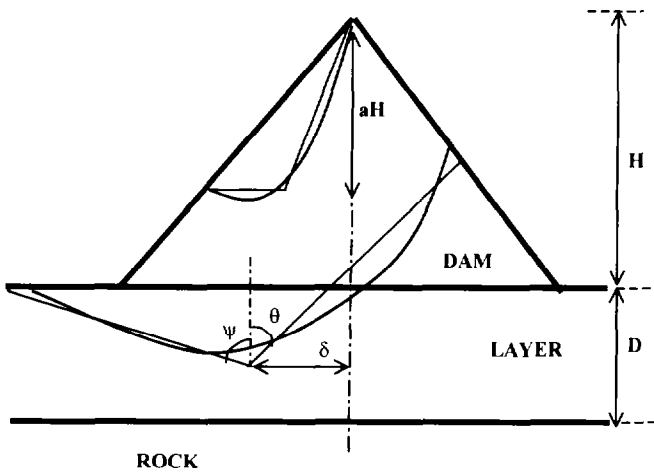


Fig. 2: Geometry of pre-defined failure surfaces.

Strong motions used in the analysis

In total 128 strong motion histories (two horizontal components of 64 strong motion recordings) from earthquakes all over the world have been used as the input in the dam response analyses. The records have been selected according to the following criteria: (a) the instrument has been sheltered in a 'free-field' station, (b) the station's geology is classified as 'rock', (c) the peak ground acceleration (PGA) of at least one of the two horizontal components is greater than $0.1g$ as records with smaller values of PGA are not of engineering significance. Figure 3, shows the distribution of the dataset in terms of surface wave magnitude, M_s , and source distance. The source distance is defined as the closest distance, d_f , from the surface projection of the causative fault; these cases are

plotted as points in Fig. 3. Where a value for d_f is not available, the epicentral distance has been used; these cases are plotted as crosses in Fig. 3. All the strong motion records are from shallow crustal earthquakes, with the deepest earthquake having a focal depth of 17 km.

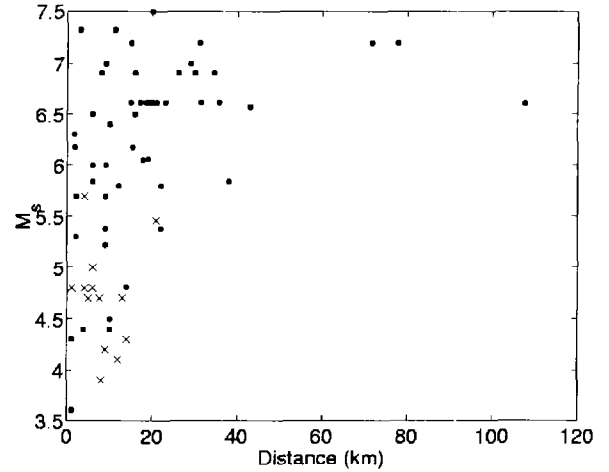


Fig. 3. Distribution of earthquake dataset used in the analysis in terms of surface magnitude, M_s and 'source distance', d . For definition of d , see text.

Results

The response analysis has been performed for a number of different dam-layer configurations and damping values, λ , with the dam having a slope angle of H:V=3:1. For this purpose two new parameters, m and R , are introduced: m is the ratio of dam-layer stiffnesses given by $m = S_D \rho_D / S_L \rho_L$ where S and ρ denote shear wave velocity and density and R is given by $R = D \rho_D / H \rho_D$ with D and H denoting the layer thickness and dam height. If it is assumed that dam and layer have the same density, then m and R become ratios of shear wave velocities and height between dam and layer. The following parameters values have been used: $m=0$ (Rigid Base), 0.2, 0.5, 1; $R = 0.1, 0.25, 0.5, 1$; $\lambda=5\%, 10\%, 20\%$ of critical damping. For each set of values of m, R and λ , values, seismic coefficients for 1-parameter failure wedges extending to depths of $y/H=0.2, 0.4, 0.6, 0.8, 1$, have been calculated for dam periods ranging from 0.1 to 2 sec. The results are presented in the form of seismic coefficient spectra. Figure 4 shows the spectrum for the rigid base case ($m=0$) and a damping value of 10%. Figure (4a) plots the average value, μ of the seismic coefficient k from all 123 strong motion histories (plotted as crosses); Fig. (4b) plots the variation of these values in terms of their standard deviation, σ_a and Fig.(4c) plots a 'standard error' term, e , defined as $e = (\mu + \sigma_a) / \mu$; this is to be used for the direct comparison of this method with the attenuation relations derived, as explained later.

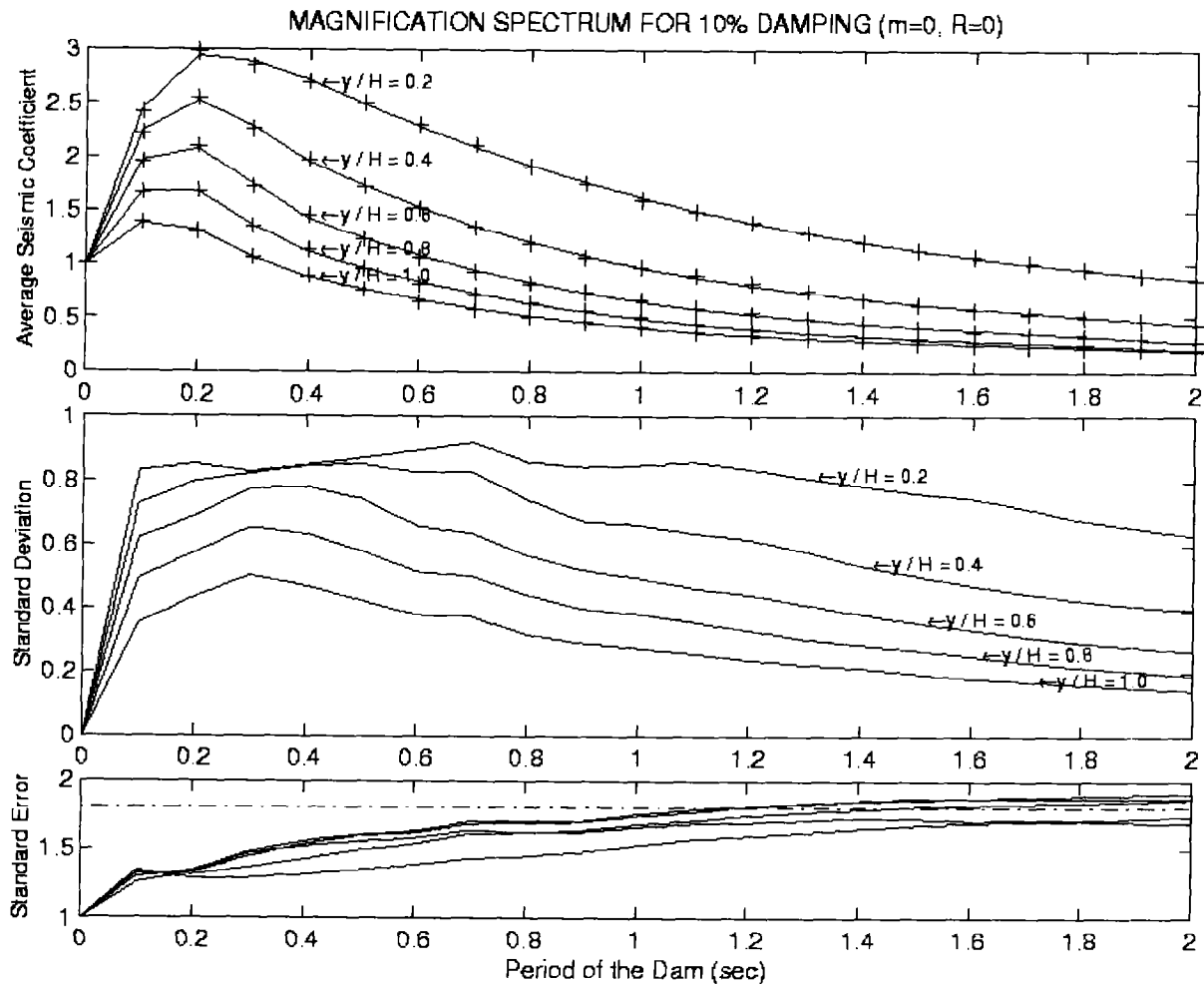


Fig. 4 : Seismic coefficient spectra and statistics for rigid base (Damping = 10%).
 (a): Average Seismic Coefficient, (b): Standard Deviation, (c): Standard error

The results of the seismic response analysis for the range of values of m and R considered were compared with the rigid base case and the following have been observed:

- a. The flexible layer influences the response of the system only when its depth is comparable to the height of the dam. For values of R less than 0.1 the response is invariable to the value of m . Figure 5 plots the seismic coefficient spectra for a sliding wedge of depth $0.2 y/H$, for $R=0.1$, damping of 5% and a range of m values.
- b. For values of R less than 0.5 extreme m value cases ($m=0.1$, $m=1$) will give similar results, particularly for high dam periods ($T \geq 1$ sec) and compare with the rigid base solution. For the $m=0.1$ case it is obvious why this happens. For the $m=1$ case this can be explained if one thinks of the dam-layer system as a rigid base case with modified geometry. The highest 'magnification' of the seismic coefficient spectral ordinates, compared with the rigid base solution, will, occur for intermediate values of m . Fig. 6 plots the seismic coefficient spectra for a sliding wedge of depth $0.2 y/H$, for $R=0.25$, damping of 5% and a range of m values. Note in Fig. 6 the similar spectra for the $m=0$, $m=0.1$, $m=0.2$, and $m=1$ cases and the differentiation of the intermediate $m=0.5$ case. For comparison, Fig. 7,8 plot seismic coefficient spectra for $R=0.5$ and $R=1$.
- c. The increase in the spectral ordinates of the seismic coefficient is complemented with a shift of maximum spectral ordinates towards higher periods. This is more evident in Fig. 7 & 8.

It is noted that the above points and similarities are all expressed in terms of m and R for similar dam periods. It should not be forgotten that for a given dam-layer configuration the period of the dam will change with changing values of m and R .

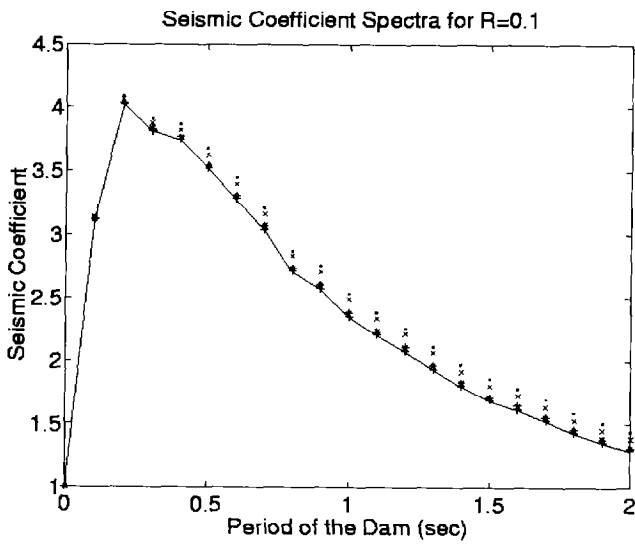


Fig. 5 : Seismic coefficient spectra for sliding wedge at depth $y/h = 0.2$, for $\lambda=5\%$. Solid line = Rigid base case ($m=0$), (+): $m=0.1$, (*): $m=0.2$, (\bullet): $m=0.5$, (x) : $m=1$.

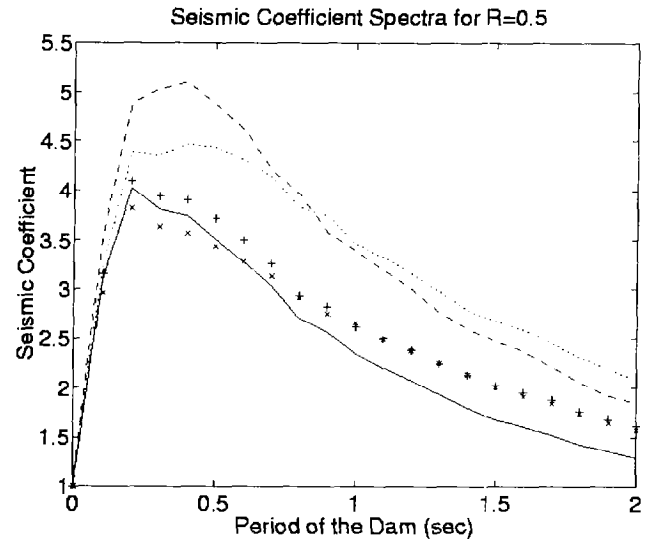


Fig. 7: Seismic coefficient spectra for sliding wedge at depth $y/h = 0.2$, for $\lambda=5\%$. Solid line = Rigid base case ($m=0$), (+): $m=0.1$, Dotted line : $m=0.2$, Dashed line : $m=0.5$, (x) : $m=1$.

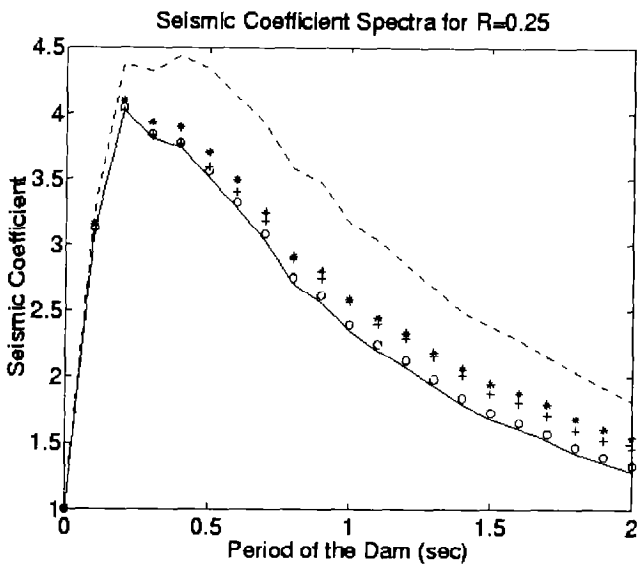


Fig. 6 : Seismic coefficient spectra for sliding wedge at depth $y/h = 0.2$, for $\lambda=5\%$. Solid line : Rigid base ($m=0$), (o) : $m=0.1$, (*) : $m=0.2$, Dashed line : $m=0.5$, (+) : $m=1$

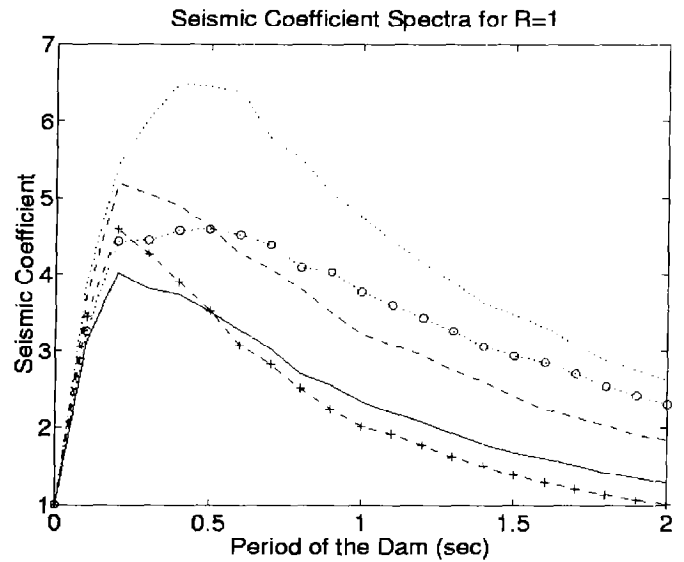


Fig. 8 : Seismic coefficient spectra for sliding wedge at depth $y/H = 0.2$, for $\lambda=5\%$. Solid line : Rigid base case ($m=0$), (-o-) : $m=0.1$, Dotted line : $m=0.2$, Dashed line : $m=0.5$, (-+-) : $m=1$.

Table 1: Regression coefficients a_1 to a_6 of equation (1) for selected cases of λ , m , R .

$\lambda(\%)$	m	R	y/h	a_1	a_2	a_3	a_4	a_5	a_6
10	0	0	0.2	20.786	-69.728	71.234	-2.402	1.090	-0.196
10	0	0	0.4	18.649	-69.875	72.992	-2.394	1.480	-0.359
10	0	0	0.6	15.465	-65.174	72.931	-1.967	1.341	-0.350
10	0	0	0.8	11.228	-51.408	60.093	-1.591	1.108	-0.291
10	0	0	1	6.979	-35.710	43.768	-1.213	0.849	-0.223
10	0.2	0.5	0.2	21.470	-67.260	67.470	-1.755	0.223	0.084
10	0.2	0.5	0.4	19.312	-69.679	71.141	-2.297	1.336	-0.320
10	0.2	0.5	0.6	16.221	-66.796	73.854	-1.899	1.260	-0.332
10	0.2	0.5	0.8	11.920	-53.133	61.194	-1.496	0.998	-0.262
10	0.2	0.5	1	7.627	-37.412	45.071	-1.143	0.748	-0.194
10	0.5	0.5	0.2	24.019	-71.483	68.871	-2.813	1.043	-0.135
10	0.5	0.5	0.4	21.396	-71.066	69.323	-2.972	1.740	-0.406
10	0.5	0.5	0.6	18.446	-70.481	74.308	-2.407	1.578	-0.403
10	0.5	0.5	0.8	14.912	-63.546	71.908	-1.879	1.242	-0.316
10	0.5	0.5	1	10.825	-49.384	57.931	-1.577	1.076	-0.279

A dichotomous third order regression equation of the form

$$k=1+a_1T+a_2T^2+a_3T^3 \quad (1a)$$

for $T \leq T_c$ and

$$k=1+a_1T_c+a_2T_c^2+a_3T_c^3+a_4(T-T_c)+a_5(T-T_c)^2+a_6(T-T_c)^3 \quad (1b)$$

for $T \geq T_c$

has been fitted to the seismic coefficient spectra. T is the fundamental period of the dam and T_c is a 'critical period' chosen so as to minimize the residual of the regression. For almost all cases $T_c = 0.4$ gives the optimum solution and this value is therefore adopted. In Fig. (4a) regression equation (1) is plotted as solid lines. Table 1 shows values of regression coefficients a_1 to a_6 for selected cases of m , R values, for a damping coefficient of 10% of critical; space limitations do not allow presentation of the whole set of data. It can be seen from Fig. (4a) that the dichotomous regression model fits the data exceptionally well.

ATTENUATION OF DAM ACCELERATIONS

The seismic coefficient method can be used to calculate the earthquake induced accelerations in the dam provided that the design peak ground acceleration at the site is known. An alternative method would be to derive a predictive attenuation relationship of peak accelerations along the height of the dam in terms of earthquake magnitude, source distance, and focal depth. Predictive attenuation relationships are of the form

$$\log(X) = a + bM + c \log(r) + dr + \sigma P \quad (2)$$

where X is the dependent parameter, M is the magnitude, r is a distance term given by $r = \sqrt{d^2 + h^2}$, d is the source term, h is a 'depth' term to be evaluated from the analysis, σ is the 'standard error' of the parameter X given from the attenuation equation and P is a constant that depends on the value of percentiles being considered in equation (2). Attenuation coefficients have been calculated for each set of m , R , λ , T and y/H values. Details of the variation of the coefficients with different parameters will not be given here. The two methods can be compared in terms of their scatter. Figure 8 shows a histogram of the 'standard error' of the derived attenuation relations for all cases. It can be seen that more than 80% of the attenuation relationships have a scatter of more than 1.8. For comparison the standard error of the seismic coefficients shown in Fig. (4c) hardly exceeds 1.8 for the whole range of periods and this only on the high period range. Furthermore, for the critical wedge extending to a depth of 0.2 y/H , the standard error never exceeds 1.8 even for the high periods (this is the bottom curve of Fig. 4c). It is therefore argued that due to the smaller scatter, the magnification curves of seismic coefficients are preferred over the attenuation relationships.

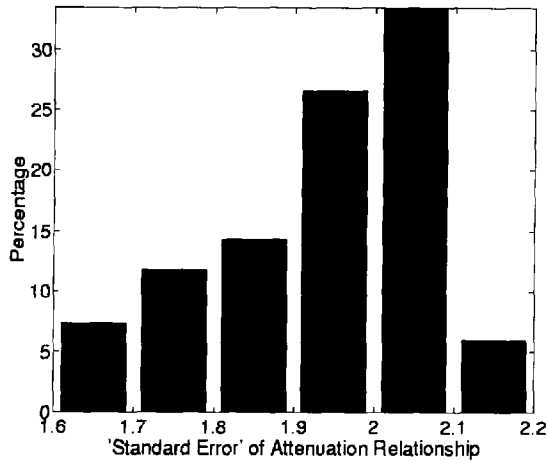


Fig 9: Variation of scatter of attenuation relationships.

PERMANENT GROUND DISPLACEMENTS

The earthquake-induced displacements, for all values of m , R , y/H and λ have been calculated for a sliding wedge of depth $0.2 y/H$ from the top of the dam. The input motion is the response time history of the wedge and a modified Newmark type rigid-block sliding model (Sarma, 1975) has been used for the analysis. The two main factors affecting the size of the calculated displacements are the period of the dam, T and the 'critical acceleration ratio', k_c/k_m where k_c is the 'critical' seismic coefficient which would bring the dam slope to a state of limiting equilibrium and k_m is the maximum seismic coefficient defined as $k_m = a_{max}/g$ where a_{max} is the maximum acceleration of the response time history. The effect of the other parameters is inherit in the response time history.

The displacement data has been binned in terms of T and k_c/k_m . Figures 10 and 11 plot the mean value and 'standard error' term, defined as $(\mu+\sigma)/\mu$ for each set of data. As expected, for a given value of k_c/k_m , displacements increase with increasing values of T .

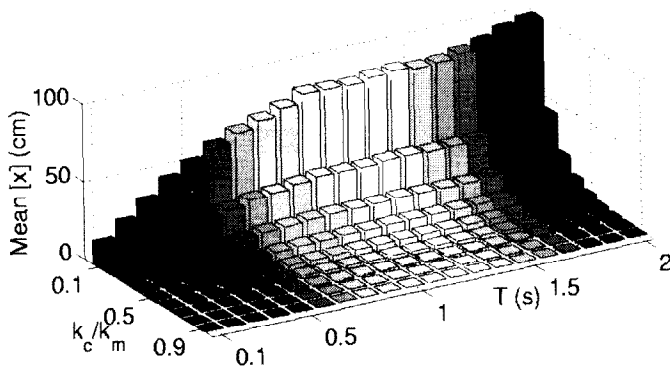


Fig. 10. Mean value of earthquake induced displacements

A number of researchers have studied the problem of earthquake-induced displacements in the past and have produced expressions for average and upper bound values. Most of these studies have used ground strong motions as the input motion in the analysis. Ambraseys (1972) produced an upper bound solution given by:

$$\log(u) = 2.3 - 3.3 k_c/k_m \quad (3)$$

where u is the displacement. When the original strong motion records are used as the input motion in the displacements analysis, equation (3) fits the data well. However when the dam response strong motions are used as the input motion, the upper bound displacement values can be more than an order of magnitude higher due to the higher accelerations (magnification effect) and the higher periods of the response records (Fig. 12)

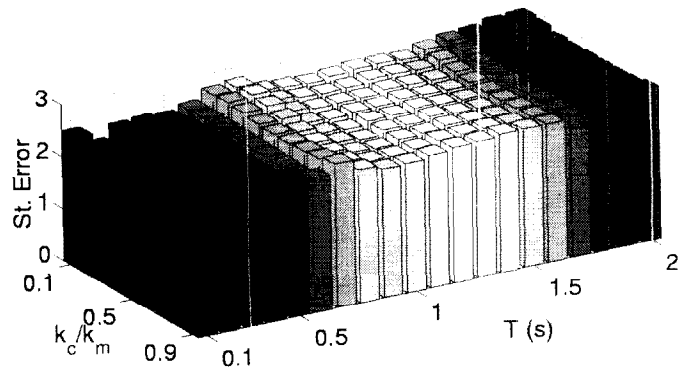


Fig. 11. Scatter of earthquake induced displacements.

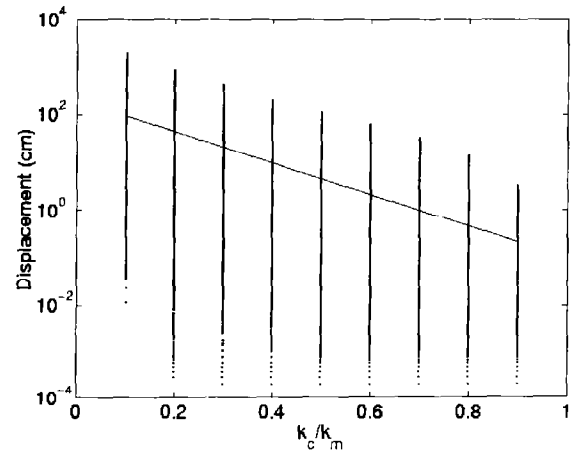


Fig. 12 : Permanent earthquake induced displacements from dam response analysis. Straight line given from equation (3).

Sarma (1975) reduced the inherent scatter in the data by plotting the dimensionless quantity $[4x_m / k_m g T_p^2]$, where x_m is the displacement and T_p is the predominant period from the acceleration spectrum of the record. An upper bound of this

form is given by Sarma (1981) as :

$$\log \left[\frac{1}{c} \frac{4x_m}{k_m g T_p^2} \right] = 1.07 - 3.83 \frac{k_c}{k_m} \quad (4)$$

where x_m is the displacement, T is the predominant period of the acceleration record, c is a function of the slope angle, the angle of shear resistance of the material and the direction of application of the inertia force. In the present study a similar plot is produced, with T_p the predominant period of the dam. If the response of the dam was wholly dominated by the fundamental mode, then the scatter would reduce. However it is seen that this is not the case and the use of T does not improve the scatter, which implies a significant contribution from the other modes in the response.

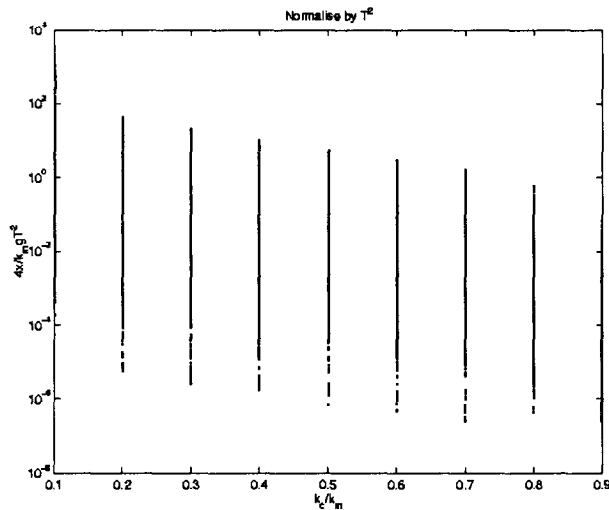


Fig. 13: Plot of $4u/k_m g T^2$ with k_c/k_m for all data.

Extreme values distribution

It is usually the case that the practising engineer is interested in the maximum values of permanent displacements that can be attained for specific values of parameters such as T or k_c/k_m . An extreme value probability distribution of the calculated displacements is therefore a useful tool that can be

used to assess the magnitude of the permanent displacements within acceptable 'confidence' limits. A Weibull distribution with a lower limit equal to zero fits the data quite well. The probability density function, $f(x)$, of the Weibull distribution is given by :

$$f(x) = abx^{b-1} e^{-ax} \quad (5)$$

with a and b both positive. The permanent displacements were classified into 180 sets for all combinations of T and k_c/k_m and for each set of data, the parameters a and b of the fitted Weibull distribution were calculated and are shown in Table 2. Having calculated parameters a and b one can use the inverse Weibull distribution,

$$u = \left[\frac{1}{a} \ln \left(\frac{1}{1-p} \right) \right]^{1/b} \quad (6)$$

to calculate extreme values of displacement, u , for a probability of non-exceedence p . Table 2 shows permanent displacement values for probabilities of exceedence of, 20% and 5%.

The variation of the Weibull parameters a and b has been investigated through a multiple regression rendered linear through an appropriate logarithmic transformation. The method is the same as adopted by Ambraseys & Menu (1988) although in the present study the period of the dam, T has also been included in the regression.

For the whole set of data the regression analysis gives :

$$a = 0.264 (k_c/k_m)^{0.689} (1 - k_c/k_m)^{-1.575} T^{-0.407} \quad (7)$$

$$b = 0.685 (k_c/k_m)^{0.017} T^{-0.156} \quad (8)$$

A regression analysis of b including the term $(1 - k_c/k_m)$ was also performed but its inclusion did not improve the fit. Equations (7) and (8) have multiple correlation coefficient values, R^2 , of 0.96 and 0.86 respectively.

Table 2: Average and extreme values of earthquake induced displacements for different values of T and k_c/k_m . Columns 3 and 4 give the average value, μ of displacement (in cm) and the 'standard error' term, $(\mu+\sigma)/\mu$. Columns 5 to 8 give Weibull parameters a and b and predicted values of permanent displacements, in cm, for probabilities of exceedence, p , of 20 and 5 per cent.

T (s)	k_c/k_m	μ (cm)	$(\mu+\sigma)/\mu$	a	b	p=20%	p=5%
0.1	0.1	15.353	2.503	0.104	0.858	24.344	50.241
	0.2	5.467	2.198	0.201	0.956	8.788	16.83
	0.3	2.372	2.132	0.41	1.02	3.818	7.02
	0.4	1.085	2.107	0.889	1.066	1.744	3.124

	0.5	0.498	2.107	2.051	1.092	0.801	1.414
	0.7	0.086	2.17	12.767	1.047	0.138	0.251
	0.9	0.004	2.533	64.925	0.707	0.005	0.013
0.5	0.1	54.494	2.451	0.069	0.71	83.677	200.682
	0.2	24.493	2.499	0.127	0.701	37.362	90.657
	0.3	12.227	2.506	0.204	0.706	18.678	45.02
	0.4	6.236	2.488	0.318	0.718	9.58	22.763
	0.5	3.106	2.462	0.511	0.732	4.798	11.216
	0.7	0.632	2.438	1.63	0.757	0.984	2.236
	0.9	0.04	2.64	11.919	0.716	0.061	0.145
1	0.1	84.52	2.591	0.073	0.64	124.462	328.661
	0.2	36.543	2.569	0.13	0.631	53.764	143.943
	0.3	17.415	2.532	0.199	0.642	25.905	68.171
	0.4	8.605	2.489	0.297	0.659	12.965	33.285
	0.5	4.27	2.459	0.453	0.677	6.504	16.288
	0.7	0.911	2.434	1.269	0.701	1.404	3.406
	0.9	0.064	2.491	8.019	0.692	0.098	0.241
1.5	0.1	85.275	2.633	0.068	0.654	125.6	324.702
	0.2	36.697	2.613	0.127	0.638	53.776	142.387
	0.3	17.997	2.585	0.199	0.638	26.522	70.238
	0.4	9.238	2.566	0.298	0.644	13.722	36.015
	0.5	4.787	2.554	0.447	0.651	7.163	18.616
	0.7	1.104	2.567	1.156	0.653	1.661	4.3
	0.9	0.084	2.65	6.062	0.637	0.125	0.331
2	0.1	99.597	2.943	0.07	0.633	140.992	376.044
	0.2	43.494	2.922	0.127	0.617	61.185	167.483
	0.3	21.229	2.841	0.196	0.617	30.214	82.669
	0.4	10.952	2.82	0.292	0.62	15.706	42.764
	0.5	5.758	2.831	0.436	0.618	8.263	22.569
	0.7	1.363	2.833	1.068	0.611	1.958	5.416
	0.9	0.11	2.922	4.808	0.587	0.155	0.447

CONCLUSIONS

The spectra of average seismic coefficients can be easily used in the seismic design of earth dams. The scatter in the displacement values is significant and depends on the variability of the strong motions; an extreme value distribution (Weibull) will give expected displacements within 'confidence' limits. The sliding block displacements using the response accelerations may be one order of magnitude different from that computed using the ground motions.

ACKNOWLEDGEMENTS

The present paper is part of a research program supported by EPSRC Grant No. GR/M80741. The financial support of the 'Alexander S. Onassis' Public Benefit Foundation is also acknowledged. The assistance of Prof. N. Ambraseys and Dr. P.Smit with the strong motion records database and J.Douglas with programming is gratefully acknowledged.

REFERENCES

- Ambraseys, N.N. [1960]. The seismic stability of earth dams, *Proc. 2nd World Conf. On Earthq. Eng.*, Tokyo, pp. 1345-1363
- Ambraseys, N. N. [1972]. Behaviour of foundation materials during strong earthquakes. *Proc. 4th Eur. Symp. Earthq. Eng.*, London, 7, pp. 11-12.
- Ambraseys, N.N. and Sarma, S.K. [1967]. The response of earth dams to strong earthquakes, *Geotechnique*, 17, pp.181-213.
- Ambraseys N.N. and Menu, J.M. [1988]. Earthquake induced displacements. *Eq. Eng. & Struct. Dyn.*, 16, pp. 985-1006.
- Sarma, S. K. [1979]. Response and stability of earth dams to strong earthquakes. *Misc. Paper GL-79-13, Geot. Lab., US Army Engineers Waterways Experiment Station, Miss. USA*
- Sarma, S.K. [1981]. A simplified method for the earthquake resistant design of earth dams. *Proc. of ICE Conf. On Dams and Earthquakes*, Thomas Telford, London, pp. 156-160.